

diglyme rings occupy relatively large holes in the structure.²⁶ When corrected for thermal motion, the bond lengths in the diglyme molecule approach or exceed expected C–C and C–O bond lengths, depending upon the model chosen.²⁷

Acknowledgment. We thank Professor A. Streitwieser, Jr., for his helpful discussion and interest. We gratefully acknowledge the financial support of the National Science Foundation (through Grants GP-

(26) The potassium atom and the center of the triangle of oxygens are almost in the xz plane. The molecules pack on a layer structure. The dihedral angles between the ring and the xy , xz , and yz planes are 70.5, 87.3, and 22.5°, respectively. The ring axis forms angles of 19.8, 111.7, and 92.8° with the x , y , and z axes, respectively.

(27) W. R. Busing, K. O. Martin, and H. A. Levy, "ORFFE, a Fortran Crystallographic Function and Error Program," ORNL-TM-306, Oak Ridge National Laboratory, Oak Ridge, Tenn., 1964; W. R. Busing and H. A. Levy, *Acta Crystallogr.*, **17**, 142 (1964).

29764 and GP-36977X) and the donors of the Petroleum Research Fund, administered by the American Chemical Society, for partial support of this research. We thank Professor G. T. Seaborg and the U. S. Atomic Energy Commission for access to the Lawrence Berkeley Laboratory Computer Center.

Supplementary Material Available. Tables III (observed and calculated structure factors), IV (rms amplitudes of vibration), V (calculated hydrogen atom positions and thermal parameters), VI (bond lengths), VII (bond angles), and VIII (least-squares planes parameters) will appear following these pages in the microfilm edition of this volume of the journal. Photocopies of the supplementary material from this paper only or microfiche (105 × 148 mm, 24× reduction, negatives) containing all of the supplementary material for the papers in this issue may be obtained from the Journals Department, American Chemical Society, 1155 16th St., N.W., Washington, D. C. 20036. Remit check or money order for \$4.00 for photocopy or \$2.00 for microfiche, referring to code number JACS-74-1348.

Magnetic Circular Dichroism Spectra of Some Tetrahedral Cobalt(II) Complexes

Hajime Katô* and Katsuhiko Akimoto

Contribution from the Department of Chemistry, Faculty of Science, Kobe University, Nada-ku, Kobe 657, Japan. Received June 26, 1973

Abstract: Magnetic circular dichroism (MCD) spectra of tetrahedral cobalt(II) ions, $\text{Co}(\text{NCS})_4^{2-}$, $\text{Co}(\text{TBPO})_4^{2+}$, $\text{Co}(\text{Ph}_3\text{PO})_4^{2+}$, $\text{Co}(\text{Ph}_3\text{P})_2\text{X}_2$, and $\text{Co}(\text{Ph}_3\text{PO})_2\text{X}_2$ ($\text{X} = \text{Cl}, \text{Br}, \text{I}, \text{SCN}$), have been measured in solution. A clear assignment of almost all bands of $\text{Co}(\text{Ph}_3\text{PO})_2\text{Br}_2$ is made by analysis based on the assumption that the cobalt(II) ion is in the tetrahedral ligand field whose properties are a numerical average of those of the actual ligands. The temperature-dependence experiments have proved that the major contribution to MCD is derived from the C term. This is consistent with the previous studies on the MCD of tetrahalide cobalt(II) ions and also with the present assignment. It seems that the effect of low symmetry components in the ligand field upon the MCD is smaller than the effect of the spin-orbit coupling upon the MCD. We extend the assignment to the other cobalt(II) complexes.

The magnetic circular dichroism (MCD) spectra of a number of transition metal complexes have been measured and analyzed, and the MCD technique has been found useful in clarifying spectroscopic assignment and characterizing the symmetry of transitions.¹⁻⁵ The MCD of tetrahalide complexes of cobalt(II) has been studied in detail by many investigators.⁶⁻¹³ The signs and magnitudes of the MCD were used to make

a clear assignment of bands. The source of the MCD was found to be the temperature-dependent C term whose origin lies in the Zeeman splitting of the ground state.^{10,13} At the present time it appears that the application of the MCD studies to the other tetrahedral complexes of cobalt(II) would be of great interest.

Absorption spectra and magnetic susceptibilities have been reported for some tetrahedral and pseudo-tetrahedral complexes of cobalt(II) of the type CoL_4 , CoL_2X_2 , CoLX_3 , and CoX_4 , and the analyses and interpretations of these data have been discussed.¹⁴⁻²³ The

* Author to whom correspondence should be addressed; Ramsay Fellow.

(1) A. D. Buckingham and P. J. Stephens, *Annu. Rev. Phys. Chem.*, **17**, 399 (1966).

(2) P. N. Schatz and A. J. McCaffery, *Quart. Rev., Chem. Soc.*, **23**, 552 (1969).

(3) "Magneto Optical Effects," *Symp. Faraday Soc.*, No. 3 (1969), and references cited therein.

(4) H. Katô, *J. Chem. Phys.*, **58**, 1964 (1973).

(5) H. Katô, *Mol. Phys.*, **24**, 81 (1972).

(6) S. H. Lin and H. Eyring, *J. Chem. Phys.*, **42**, 1780 (1965).

(7) P. J. Stephens, *ibid.*, **43**, 4444 (1965).

(8) R. G. Denning, *ibid.*, **45**, 1307 (1966).

(9) B. D. Bird, B. Briat, P. Day, and J. C. Rivoal, *Symp. Faraday Soc.*, No. 3, 70 (1969).

(10) R. G. Denning and J. A. Spencer, *ibid.*, No. 3, 84 (1969).

(11) J. A. Lomenzo, B. D. Bird, G. A. Osborne, and P. J. Stephens, *Chem. Phys. Lett.*, **9**, 332 (1971).

(12) J. C. Collingwood, P. Day, and R. G. Denning, *ibid.*, **10**, 274 (1971).

(13) B. D. Bird, J. C. Collingwood, P. Day, and R. G. Denning, *Chem. Commun.*, 225 (1971).

(14) N. M. Karayannis, C. M. Mikulski, L. L. Pytlewski, and M. M. Labes, *Inorg. Chem.*, **9**, 582 (1970).

(15) F. A. Cotton, D. M. L. Goodgame, and M. Goodgame, *J. Amer. Chem. Soc.*, **83**, 4690 (1961).

(16) D. M. L. Goodgame and M. Goodgame, *Inorg. Chem.*, **4**, 139 (1965).

(17) R. H. Holm and F. A. Cotton, *J. Chem. Phys.*, **31**, 788 (1959); **32**, 1168 (1960).

(18) F. A. Cotton and M. Goodgame, *J. Amer. Chem. Soc.*, **83**, 1777 (1961).

(19) F. A. Cotton, O. D. Faut, D. M. L. Goodgame, and R. H. Holm, *ibid.*, **83**, 1780 (1961).

(20) F. A. Cotton, D. M. L. Goodgame, M. Goodgame, and A. Sacco, *ibid.*, **83**, 4157 (1961).

(21) J. Ferguson, *J. Chem. Phys.*, **39**, 116 (1963).

(22) B. D. Bird and P. Day, *ibid.*, **49**, 392 (1968).

(23) J. Ferguson, D. L. Wood, and L. G. Van Uitert, *ibid.*, **51**, 2904 (1969).

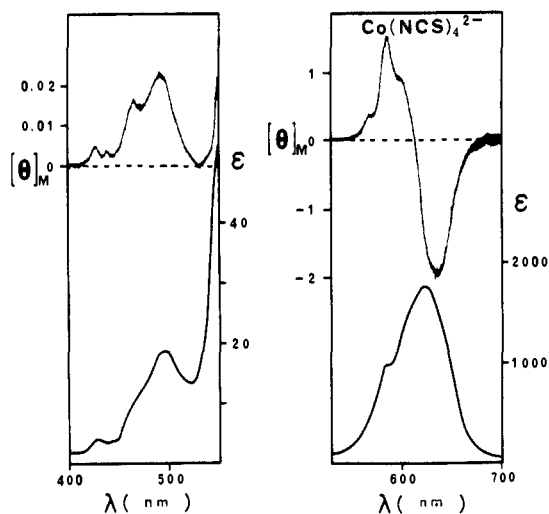


Figure 1. MCD and absorption spectra of $\text{Co}(\text{NCS})_4^{2-}$ in CH_2Cl_2 at room temperature. $[\theta]_M$ is the molar ellipticity per unit magnetic field. ϵ is the molar extinction coefficient.

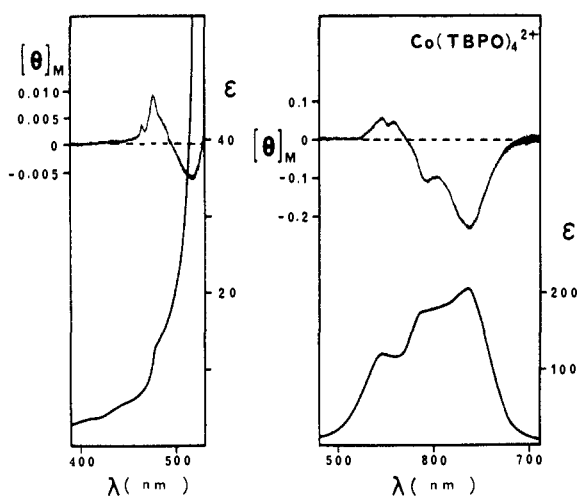


Figure 2. MCD and absorption spectra of $\text{Co}(\text{TBPO})_4^{2+}$ in CH_2Cl_2 at room temperature.

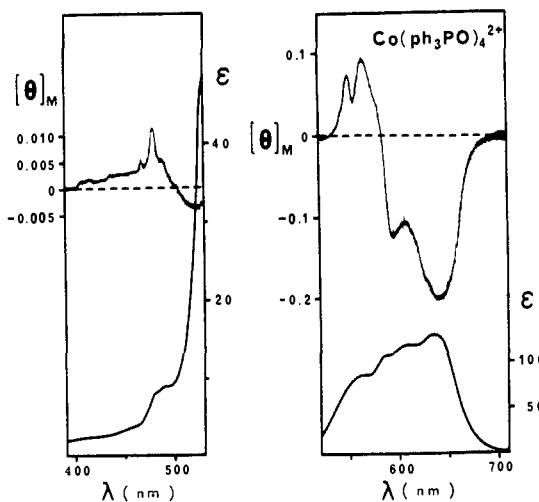


Figure 3. MCD and absorption spectra of $\text{Co}(\text{Ph}_3\text{PO})_4^{2+}$ in CH_2Cl_2 at room temperature.

absorption spectra measured at room temperature using mulls and solutions are handicapped by poor resolution. However, the MCD spectrum through

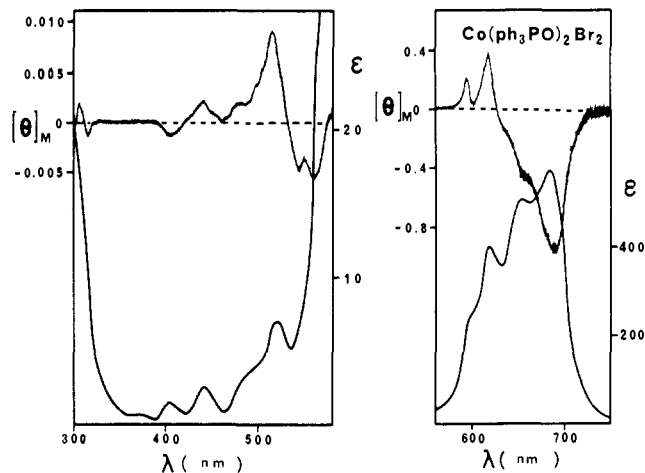


Figure 4. MCD and absorption spectra of $\text{Co}(\text{Ph}_3\text{PO})_2\text{Br}_2$ in CH_2Cl_2 at room temperature.

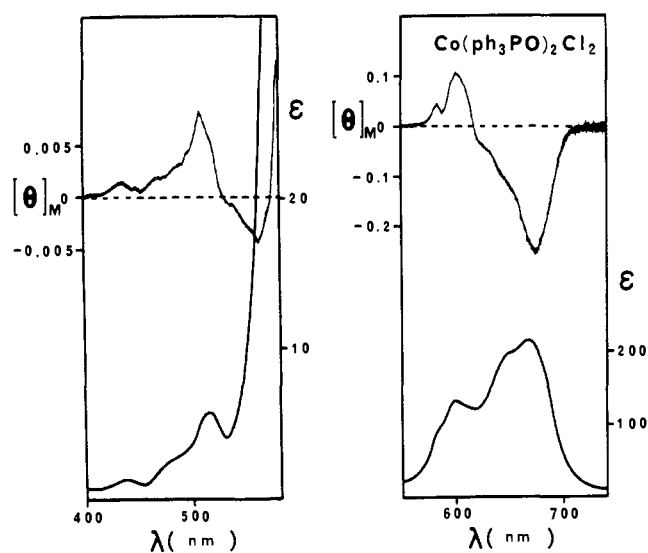


Figure 5. MCD and absorption spectra of $\text{Co}(\text{Ph}_3\text{PO})_2\text{Cl}_2$ in CH_2Cl_2 at room temperature.

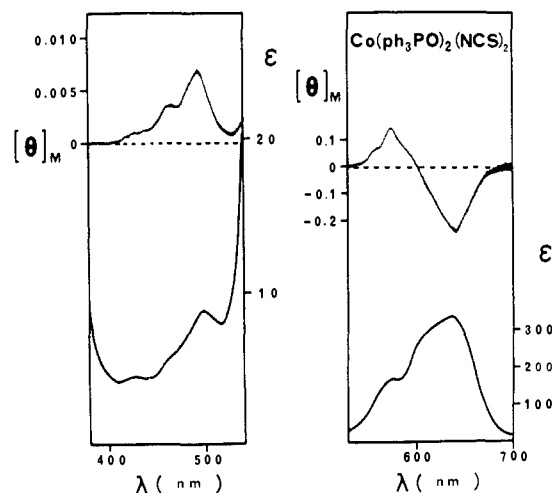


Figure 6. MCD and absorption spectra of $\text{Co}(\text{Ph}_3\text{PO})_2(\text{NCS})_2$ in CH_2Cl_2 at room temperature.

an absorption band can provide information not available from the absorption spectrum. In the case where

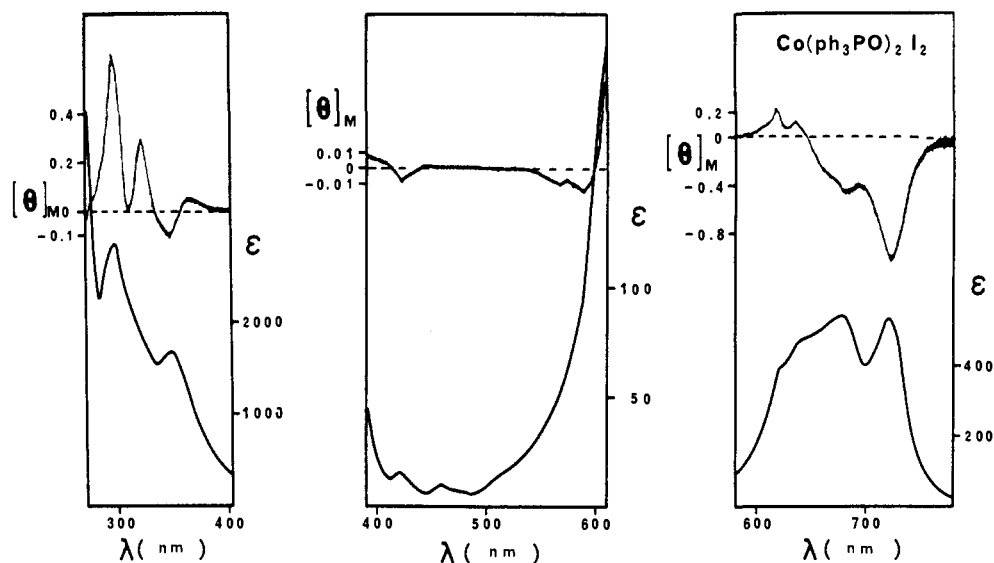


Figure 7. MCD and absorption spectra of $\text{Co}(\text{Ph}_3\text{PO})_2\text{I}_2$ in CH_2Cl_2 at room temperature.

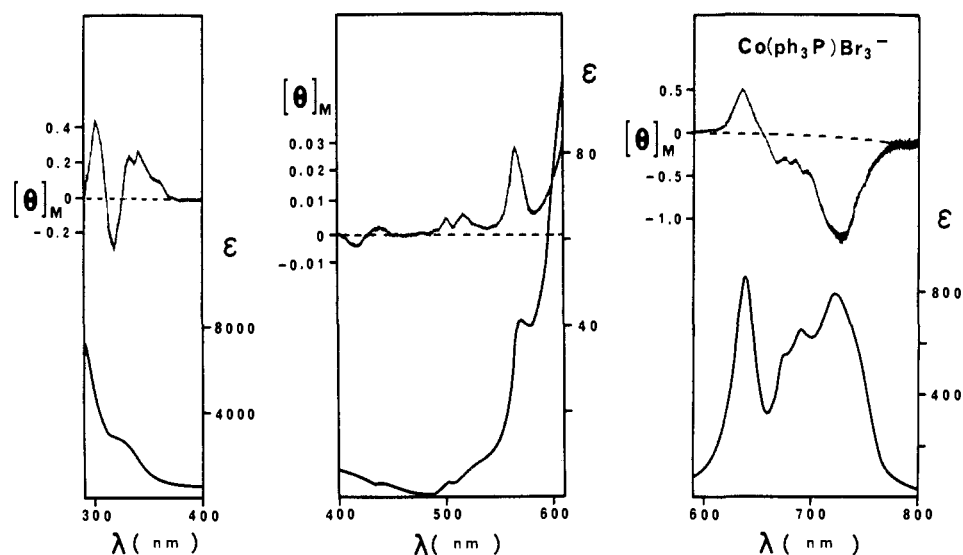


Figure 8. MCD and absorption spectra of $\text{Co}(\text{Ph}_3\text{P})\text{Br}_3^-$ in CH_2Cl_2 at room temperature.

the ground state is spin-degenerate and orbitally non-degenerate, the spin-forbidden transitions are expected to show huge MCD,^{4,24,25} and the assignment of these transitions is greatly facilitated. In the present paper, we will report new MCD data for some cobalt(II) complexes of the type CoL_4 , CoL_2X_2 , CoLX_3 , and CoX_4 and discuss the electronic structures. It is also interesting to see the change of the MCD spectra accompanying the departures of the ligand symmetry from T_d .

Experimental Section

The following compounds used in this study were prepared and recrystallized according to previously reported procedures: bis(triphenylphosphine oxide)dihalocobalt(II), $\text{Co}(\text{Ph}_3\text{PO})_2\text{X}_2$ ($\text{X} = \text{Cl}, \text{Br}, \text{I}$,²⁶ NCS^{20}); bis(triphenylphosphine)dihalocobalt(II), $\text{Co}(\text{Ph}_3\text{P})_2\text{X}_2$ ($\text{X} = \text{Cl}, \text{Br}, \text{I}$,¹⁹ SCN^{20}); tetrakis(triphenylphosphine oxide)cobalt(II) perchlorate, $\text{Co}(\text{Ph}_3\text{PO})_4(\text{ClO}_4)_2$;²⁷ tetrakis(tri-*n*-butylphosphine oxide)cobalt(II) perchlorate, $\text{Co}(\text{TBPO})_4(\text{ClO}_4)_2$;¹⁴

tetramethylammonium tetrathiocyanatocobaltate(II), $[(\text{CH}_3)_4\text{N}]_2[\text{Co}(\text{NCS})_4]$;²⁰ tetraethylammonium tribromo(triphenylphosphine)cobalt(II), $[(\text{C}_2\text{H}_5)_4\text{N}][\text{Co}(\text{Ph}_3\text{P})\text{Br}_3]$.¹⁹

The absorption and MCD spectra at room temperature were measured by the techniques described in detail in earlier papers.^{5,26} The results are presented in Figures 1–12. In order to show the signal-to-noise ratio of a dichrometer, the observed MCD spectra are shown just as is. In order to measure the absorption and MCD spectra of a sample in solution at lower temperatures, we used a simple cryostat. It is shown in Figure 13. The sample was poured into a quartz cell with a 2.5-mm optical path, and the cell was fixed to the dewar at the upper end. The outside of the cell, the inside of the dewar, was filled with toluene whose melting point is higher than that of the solvent of the sample. It was cooled by adding liquid nitrogen, and the temperature was measured by a thermoelectric thermometer. The values of the temperature have a precision of $\pm 1^\circ\text{K}$. We measured the MCD of a solution without solute first, the trace provides the MCD base line, and then we measured the MCD with solute at room temperature. Then, with paying much attention not to move the cryostat, we measured the MCD at low temperatures. The absorption spectra were also measured in the same manner. The results for $\text{Co}(\text{Ph}_3\text{PO})_2\text{Br}_2$ are presented in Figures 14 and 15.

Discussion

The absorption bands corresponding to the transi-

(24) A. J. McCaffery, P. J. Stephens and P. N. Schatz, *Inorg. Chem.*, **6**, 1614 (1967).

(25) H. Katô, *J. Chem. Phys.*, **59**, 1732 (1973).

(26) F. A. Cotton, R. D. Barnes, and E. Bannister, *J. Chem. Soc.*, 2199 (1960).

(27) E. Bannister and F. A. Cotton, *ibid.*, 1878 (1960).

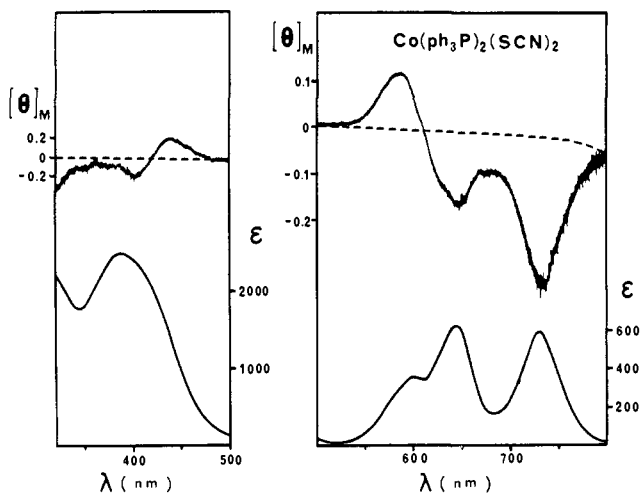


Figure 9. MCD and absorption spectra of $\text{Co}(\text{Ph}_3\text{P})_2(\text{SCN})_2$ in CH_2Cl_2 at room temperature.

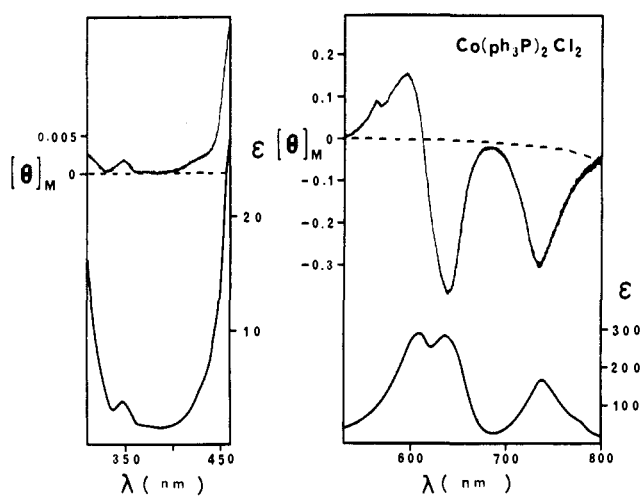


Figure 10. MCD and absorption spectra of $\text{Co}(\text{Ph}_3\text{P})_2\text{Cl}_2$ in CH_2Cl_2 at room temperature.

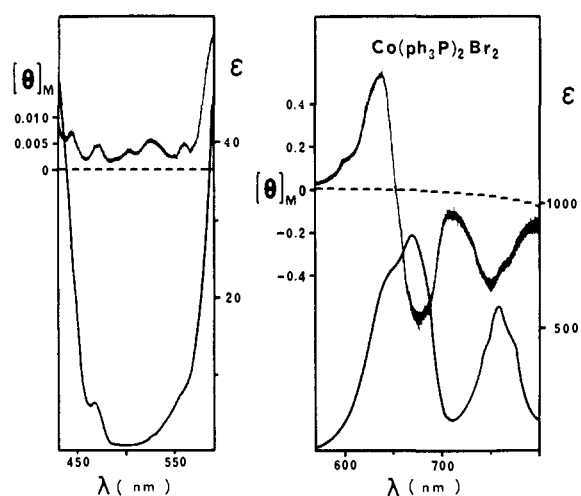


Figure 11. MCD and absorption spectra of $\text{Co}(\text{Ph}_3\text{P})_2\text{Br}_2$ in CH_2Cl_2 at room temperature.

tion ${}^4\text{A}_2 \rightarrow {}^4\text{T}_1(\text{P})$ of various tetrahedral cobalt(II) ions occur in the $13,000\text{--}18,000\text{-cm}^{-1}$ region with molar extinction coefficients of the order of magnitude $100\text{--}1000$. The ordering of ligands according to the relative

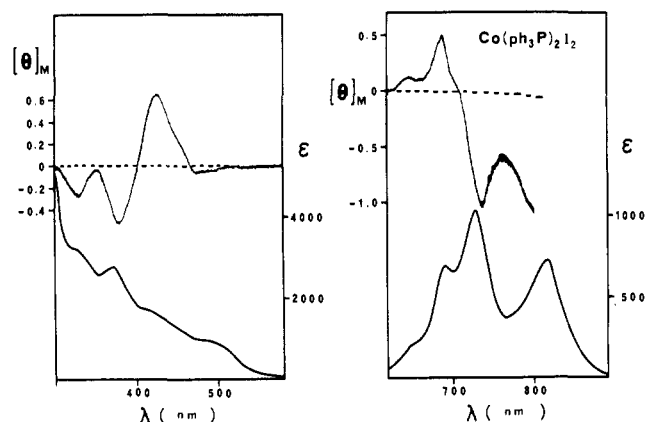


Figure 12. MCD and absorption spectra of $\text{Co}(\text{Ph}_3\text{P})_2\text{I}_2$ in CH_2Cl_2 at room temperature.

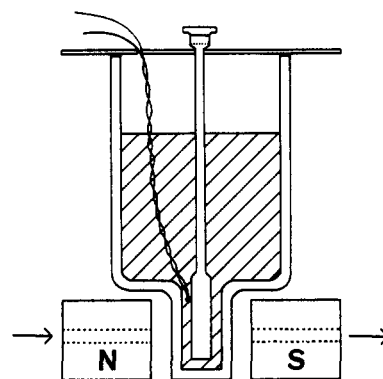


Figure 13. Schematic diagram of the cryostat used in our experiments.

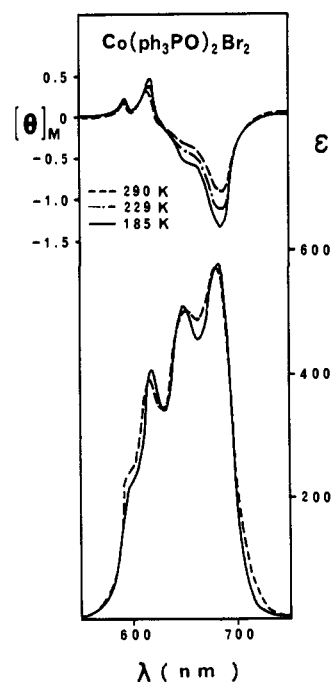


Figure 14. Temperature dependence of the MCD and absorption spectra of $\text{Co}(\text{Ph}_3\text{PO})_2\text{Br}_2$ in CH_2Cl_2 , spin-allowed transition ${}^4\text{A}_2 \rightarrow {}^4\text{T}_1(\text{P})$.

strengths of their contributions to ligand fields has been given as^{13,19} $\text{I}^- < \text{Br}^- < \text{-SCN}^- < \text{Cl}^- < \text{Ph}_3\text{PO} <$

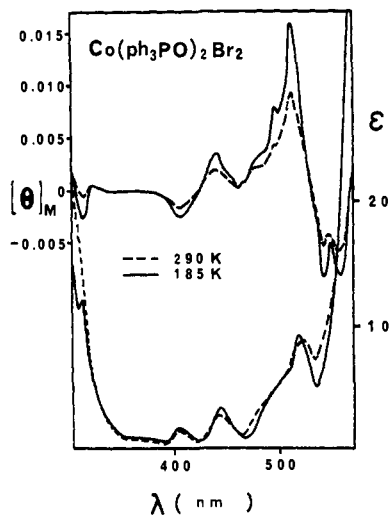


Figure 15. Temperature dependence of the MCD and absorption spectra of $\text{Co}(\text{Ph}_3\text{PO})_2\text{Br}_2$ in CH_2Cl_2 , spin-forbidden transitions.

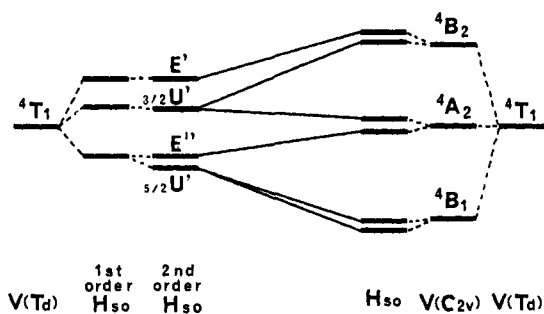


Figure 16. Schematic diagram of the spin-orbit splitting of ${}^4\text{T}_1$ state in T_d symmetry and C_{2v} symmetry ligand fields.

$\text{Ph}_3\text{P} \sim -\text{NCS}^-$. The spectrum of $\text{Co}(\text{TBPO})_4^{2+}$ shows the position of TBPO as $-\text{NCS}^- < \text{TBPO}$. The MCD and absorption spectra of the ions CoX_4^{2-} ($X = \text{Cl}, \text{Br}, \text{I}$) were measured in the region of the transition ${}^4\text{A}_2 \rightarrow {}^4\text{T}_1(\text{P})$, and the source of the MCD and the assignment of the spectra were made clear.^{8,10} The MCD spectra of the tetrahedral ions $\text{Co}(\text{NCS})_4^{2-}$, $\text{Co}(\text{TBPO})_4^{2+}$, and $\text{Co}(\text{Ph}_3\text{PO})_4^{2+}$ (Figure 1-3) are very similar to those of tetrahedral cobalt(II) ions. The main features of these spectra arise from the spin-orbit splitting of the upper state ${}^4\text{T}_1(\text{P})$ in the tetrahedral field, and the major MCD at room temperature comes from the temperature-dependent C term whose origin lies in the Zeeman splitting of the ground-state ${}^4\text{A}_2$.

In the case of complexes of the type CoL_2X_2 , the site symmetry of the cobalt(II) ions is C_{2v} , and the excited state ${}^4\text{T}_1$ in T_d symmetry is decomposed into ${}^4\text{B}_2 + {}^4\text{A}_2 + {}^4\text{B}_1$. The splitting pattern is schematically shown in Figure 16. Let us first assume that the effect of the field of lower symmetry is very small compared with the spin-orbit splitting, and the complex will be treated as though it contained identical ligands whose properties are a numerical average of those of the actual ligands (average ligand field approximation). The energy-level diagram for the cobalt(II) ion in a field of T_d symmetry is shown in Figure 17, which is obtained by diagonalizing the matrix given by Tanabe and Sugano.²⁸ We have determined the values of Dq by iden-

(28) Y. Tanabe and S. Sugano, *J. Phys. Soc. Jap.*, **9**, 753 (1954); **9**, 766 (1954).

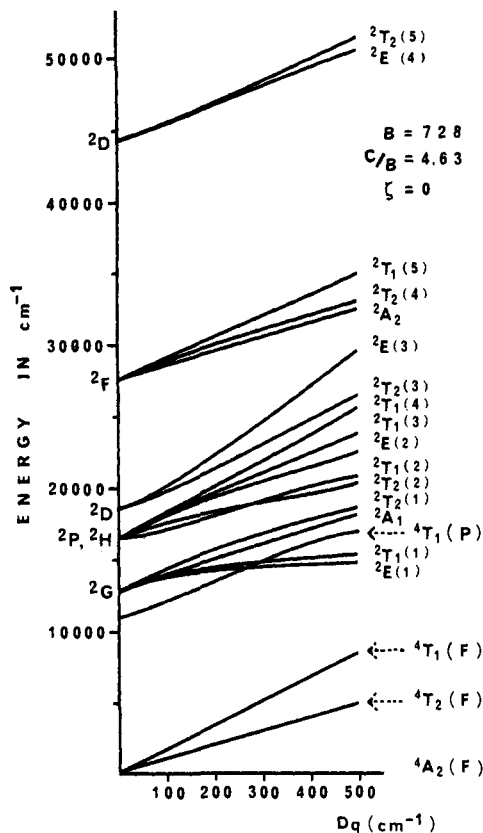


Figure 17. The energy-level diagram for the cobalt(II) ion in a field of T_d symmetry. The value of B is assumed to be 75% of the free ion and the value of C/B to be that of the free ion. The smaller values of B and C than those of the free ion were suggested by Tanabe and Sugano in ref 28.

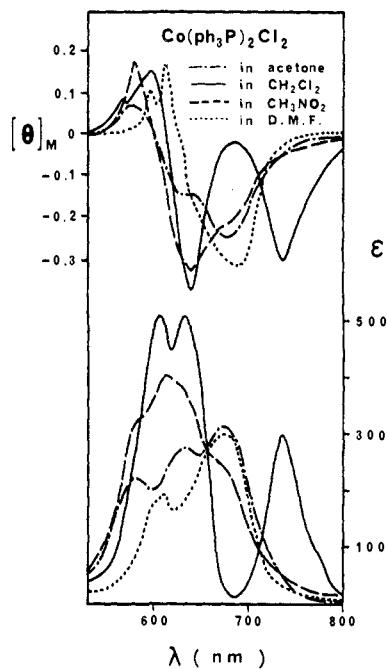


Figure 18. MCD and absorption spectra of $\text{Co}(\text{Ph}_3\text{P})_2\text{Cl}_2$ in various media.

tifying the absorption spectra with our calculated energy-level diagram (Figure 17). The results are $Dq(\text{for } \text{Co}(\text{Ph}_3\text{PO})_4^{2+}) = 455$, $Dq(\text{for } \text{CoCl}_4^{2-}) = 325$, $Dq(\text{for } \text{CoBr}_4^{2-}) = 285$, and $Dq(\text{for } \text{CoI}_4^{2-}) = 240 \text{ cm}^{-1}$.

$$\begin{vmatrix} \epsilon_3^0 + 4Dq^{ab} - \epsilon & X + 4Y & 0 & 0 & 0 \\ X + 4Y & \epsilon_3^0 + 4Dq^{ab} - \epsilon & 0 & 0 & 0 \\ 0 & 0 & \epsilon_3^0 + 4Dq^{ab} - \epsilon & -2(X - 3Y)/\sqrt{3} & 0 \\ 0 & 0 & -2(X - 3Y)/\sqrt{3} & \epsilon_3^0 - 6Dq^{ab} - \epsilon & 0 \\ 0 & 0 & 0 & 0 & \epsilon_3^0 - 6Dq^{ab} - \epsilon \end{vmatrix} = 0 \quad (1)$$

The MCD and absorption spectra of $\text{Co}(\text{Ph}_3\text{PO})_2\text{Br}_2$ (Figure 4) are in the highest resolution and seem to give us much information. Therefore, we first attempt the assignment of the d-d transitions of $\text{Co}(\text{Ph}_3\text{PO})_2\text{Br}_2$ and discuss the electronic structure. According to the average ligand field approximation, which was proposed by Cotton and his coworkers,¹⁵ the Dq value for $\text{Co}(\text{Ph}_3\text{PO})_2\text{X}_2$ complexes is supposed to be the numerical average of Dq values for CoX_4^{2-} and $\text{Co}(\text{Ph}_3\text{PO})_4^{2+}$. The Dq value for $\text{Co}(\text{Ph}_3\text{PO})_2\text{Br}_2$ is 370 cm^{-1} . Then, the calculated transition energy for ${}^4\text{A}_2 \rightarrow {}^4\text{T}_1(\text{P})$ is $15,600 \text{ cm}^{-1}$, which is in good agreement with the observed one. The MCD spectrum in the region of 600–700 nm is very similar to that observed for the CoCl_4^{2-} ion.¹⁰ Therefore we can assign the bands at 600, 620, 650, and 690 nm to the E' , $3/2\text{U}'$, E'' , and $5/2\text{U}'$ components of ${}^4\text{T}_1(\text{P})$, respectively, which are split by the spin-orbit coupling.

The most complete study of the MCD spectra for the spin-forbidden transitions of CoCl_4^{2-} was reported by Stephens and his coworkers.¹¹ Using their theoretical prediction on the sign of the MCD of each spin-forbidden transition, we shall now try to assign the MCD of the weak absorption bands between 300 and 550 nm of $\text{Co}(\text{Ph}_3\text{PO})_2\text{Br}_2$. Because of the presence of very high-intensity bands in the higher energy region than 300 nm and of our instrumental restriction, we cannot detect two doublet states ${}^2\text{T}_2(5)$ and ${}^2\text{E}(4)$ which are expected to lie in the neighborhood of 200 nm. The positive MCD band at 305 nm is assigned to ${}^4\text{A}_2 \rightarrow {}^2\text{T}_1(5)$ and the negative MCD band at 315 nm is assigned to ${}^4\text{A}_2 \rightarrow {}^2\text{T}_2(4)$, ${}^2\text{A}_2$. The absorption band at 375 nm may be assigned to ${}^4\text{A}_2 \rightarrow {}^2\text{E}(3)$, although the corresponding MCD band was not detected clearly. The negative MCD band at 405 nm is assigned to ${}^4\text{A}_2 \rightarrow {}^2\text{T}_2(3)$, the positive MCD band at 440 nm is assigned to ${}^4\text{A}_2 \rightarrow {}^2\text{T}_1(4)$, and the positive MCD band at 480 nm is assigned to ${}^4\text{A}_2 \rightarrow {}^2\text{T}_1(3)$. The band corresponding to ${}^4\text{A}_2 \rightarrow {}^2\text{E}(2)$, whose $[\theta]_{\text{M}}$ is theoretically predicted to be negative, is not detected clearly but this band will lie at the 490–500-nm region. The positive MCD band at 520 nm is assigned to ${}^4\text{A}_2 \rightarrow {}^2\text{T}_1(2)$. The negative MCD bands at 540 and 560 nm are assigned to ${}^4\text{A}_2 \rightarrow {}^2\text{T}_2(2)$ and ${}^4\text{A}_2 \rightarrow {}^2\text{T}_2(1)$, respectively. The other lower energy transitions are probably overcome by the spin-allowed ${}^4\text{A}_2 \rightarrow {}^4\text{T}_2(\text{P})$ band.

As we have seen in above, almost all bands of $\text{Co}(\text{Ph}_3\text{PO})_2\text{Br}_2$ are clearly assigned by the signs of the MCD. It is worth notice that the predicted theoretical signs of the MCD of the tetrachlorocobaltate(II) ion in T_d symmetry are in good agreement with the observed ones of $\text{Co}(\text{Ph}_3\text{PO})_2\text{Br}_2$. The transition energies of $\text{Co}(\text{Ph}_3\text{PO})_2\text{Br}_2$ are also in good agreement with the calculated ones for the cobalt(II) ion in a field of T_d symmetry (at $Dq = 370 \text{ cm}^{-1}$ in Figure 17).

Next let us assume that the effect of the field of lower symmetry is large compared with the spin-orbit splitting and the spin-orbit coupling can be treated as a perturbation on the C_{2v} symmetry field, *i.e.*, the right-hand

side of Figure 16. We consider a cobalt(II) ion surrounded by four ligands; two point charges $-Z_a e$ are at distance R_a along the $[111]$ and $[\bar{1}\bar{1}\bar{1}]$ directions, and the other two point charges $-Z_b e$ are at distance R_b along the $[1\bar{1}\bar{1}]$ and $[\bar{1}11]$ directions. According to ligand field theory, the energies of the 3d electron in the field of these charges are given by solving the secular equation 1 with definitions given in eq 2–5 where $\langle \rangle$

$$Dq^{ab} = (Z_a/R_a^5 + Z_b/R_b^5)e^2\langle r^4 \rangle / 27 \quad (2)$$

$$X = 2(Z_a/R_a^3 - Z_b/R_b^3)e^2\langle r^2 \rangle / 7 \quad (3)$$

$$Y = 10(Z_a/R_a^5 - Z_b/R_b^5)e^2\langle r^4 \rangle / 189 \quad (4)$$

$$\epsilon_3^0 = \epsilon_3 + 2e^2(Z_a/R_a + Z_b/R_b) \quad (5)$$

represents the average with respect to the radial part of the 3d function and ϵ_3 is the energy of 3d electron of the unperturbed cobalt(II) ion. The bases of the secular matrix are arranged in the order $3d_x$, $3d_y$, $3d_z$, $3d_u$, and $3d_v$. The values of $\langle r^2 \rangle$ and $\langle r^4 \rangle$ are calculated by using an analytical SCF function for the cobalt atom obtained by Clementi;²⁹ $\langle r^4 \rangle_{\text{Co}(3d)} = 4.869 a_0^4$, $\langle r^2 \rangle_{\text{Co}(3d)} = 1.495 a_0^2$. The bond distances are assumed as $R_{\text{Co-O}} = 1.95 \text{ \AA}$,³⁰ $R_{\text{Co-Cl}} = 2.28 \text{ \AA}$,³¹ $R_{\text{Co-Br}} = 2.43 \text{ \AA}$,³² $R_{\text{Co-I}} = 2.63 \text{ \AA}$,³³ which were determined by X-ray studies or other considerations. By using these values and the relationship $Dq = (2Z_a/27R_a^3)e^2\langle r^4 \rangle$, which is the crystal field splitting due to the electrostatic field created by four point charges in T_d symmetry, we can evaluate the matrix elements in eq 1. Then, the excitation energies to ${}^4\text{B}_2$, ${}^4\text{A}_2$, and ${}^4\text{B}_1$ states, which are split from ${}^4\text{T}_1(\text{P})$ in T_d symmetry by the lower symmetry field, are respectively 16,600, 15,900, and 15,100 cm^{-1} for $\text{Co}(\text{Ph}_3\text{PO})_2\text{Cl}_2$; 16,500, 15,600, and 14,700 cm^{-1} for $\text{Co}(\text{Ph}_3\text{PO})_2\text{Br}_2$; 16,600, 15,300, and 14,100 cm^{-1} for $\text{Co}(\text{Ph}_3\text{PO})_2\text{I}_2$. The magnitudes of these energy separations are satisfactory for explaining the splittings of the observed spectra.

Let us next calculate the MCD parameters for the transitions to ${}^4\text{B}_2$, ${}^4\text{A}_2$, and ${}^4\text{B}_1$ states split from ${}^4\text{T}_1(\text{P})$. The excited states ${}^4\text{B}_2$, ${}^4\text{A}_2$, and ${}^4\text{B}_1$ are further split by the spin-orbit coupling, *i.e.*, each state splits into two states, $\Gamma'(X)$ and $\Gamma''(X)$, where $X = {}^4\text{B}_2$, ${}^4\text{A}_2$, ${}^4\text{B}_1$. Assuming the spin-orbit coupling constant $\zeta = 500 \text{ cm}^{-1}$, and diagonalizing the spin-orbit coupling matrices of ${}^4\text{T}_1$ of $t_2^4({}^3\text{T}_1)e^3$ we have calculated the excitation energies and wave functions of $\text{Co}(\text{Ph}_3\text{PO})_2\text{Br}_2$. The resulting excitation energies are 16,590, 16,530, 15,640, 15,540, 14,670, and 14,630 cm^{-1} for the transitions to $\Gamma'({}^4\text{B}_2)$, $\Gamma''({}^4\text{B}_2)$, $\Gamma'({}^4\text{A}_2)$, $\Gamma''({}^4\text{A}_2)$, $\Gamma'({}^4\text{B}_1)$, and $\Gamma''({}^4\text{B}_1)$, respectively. The MCD C terms are then calculated by using the resulting wave functions, and the C/D values for each component are found to be $-0.27 \mu_B$,

(29) E. Clementi, *J. Chem. Phys.*, **41**, 295 (1964).

(30) H. A. Weakliem, *ibid.*, **36**, 2117 (1962).

(31) J. R. Wiesner, R. C. Srivastava, C. H. L. Kennard, M. DiVaira, and E. C. Lingafelter, *Acta Crystallogr.*, **23**, 565 (1967).

(32) P. Day and C. K. Jørgensen, *J. Chem. Soc., Suppl.* **2**, 6226 (1964).

(33) T. I. Malinovskii, *Kristallografiya*, **3**, 364 (1958).

$-0.21 \mu_B$, $0.03 \mu_B$, $-0.03 \mu_B$, $0.24 \mu_B$, and $0.15 \mu_B$, where μ_B is the Bohr magneton, for the transitions to $\Gamma''(^4B_2)$, $\Gamma''(^4B_2)$, $\Gamma''(^4A_2)$, $\Gamma''(^4A_2)$, $\Gamma''(^4B_1)$, and $\Gamma''(^4B_1)$, respectively. These values are smaller than the C/D values $-3/2 \mu_B$, $-1 \mu_B$, $3/2 \mu_B$, and $3/2 \mu_B$, which were predicted respectively for E' , $3/2U'$, E'' , and $5/2U'$ components of $^4T_1(P)$ in the field of T_d symmetry and were found to be the dominant contribution to the MCD of tetrahalide cobalt(II) complexes.^{10,13}

In order to compare the theoretical predictions with the observed MCD, it will be further necessary to evaluate the intrastate B terms, B' , arising from 4B_2 , 4A_2 , 4B_1 interaction. The values of B'/D for the transitions to 4B_2 , 4A_2 , and 4B_1 states are calculated to be $1/\sqrt{6}(\delta E_1 + \delta E_2) + 1/\sqrt{6}(\delta E_1)$, $-1/\sqrt{6}(\delta E_1 + \delta E_2) - 1/\sqrt{6}(\delta E_2)$, and $-1/\sqrt{6}(\delta E_1) + 1/\sqrt{6}(\delta E_2)$, respectively, in units of $\mu_B \langle ^4T_1 || I || ^4T_1 \rangle / i\hbar$ (cm^{-1}). δE_1 is the energy separation between 4B_2 and 4A_2 , and δE_2 is the energy separation between 4A_2 and 4B_1 . These values of B'/D are also smaller than the intrastate B terms predicted for E' , $3/2U'$, E'' , and $5/2U'$ components.¹⁰

As we have seen in above, we can not explain the signs and magnitudes of the MCD spectra if we assume that the effect of the field of lower symmetry is larger than that of the spin-orbit coupling. On the other hand, we have been able to yield a clear assignment of almost all of the bands of $\text{Co}(\text{Ph}_3\text{PO})_2\text{Br}_2$ on the basis of the assumption that the cobalt(II) ion is in the tetrahedral ligand field whose properties are numerical average of those of the actual ligands. The MCD spectra of $\text{Co}(\text{Ph}_3\text{PO})_2\text{Br}_2$ in both regions of the transition $^4A_2 \rightarrow ^4T_1(P)$ and the spin-forbidden transitions (Figure 14 and 15) show a remarkable variation with temperature in comparison with the absorption spectra. It is therefore evident that the dominant contributions to the MCD come from C terms, and this fact is consistent with the previous studies on the MCD of tetrahalido-cobaltate(II) ions.^{10,13} The effect of low symmetry components in the ligand field upon the MCD seems to be small in comparison with that of the spin-orbit interaction.

By using the similarity of the band shapes and the signs of MCD between $\text{Co}(\text{Ph}_3\text{PO})_2\text{Br}_2$ and the other cobalt(II) complexes, we can intuitively extend the assignment to the other cobalt(II) complexes. For $\text{Co}(\text{Ph}_3\text{PO})_2\text{Cl}_2$ (Figure 5), the positive MCD bands at 435, 470, and 515 nm and the negative MCD bands at 530 and 560 nm are assigned as the transitions to $^2T_1(4)$, $^2T_1(3)$, $^2T_1(2)$, $^2T_2(2)$, and $^2T_2(1)$, respectively. The positive MCD bands of $\text{Co}(\text{Ph}_3\text{PO})_2(\text{NCS})_2$ (Figure 6) at 430, 460, and 495 nm are assigned as the transitions to $^2T_1(4)$, $^2T_1(3)$, and $^2T_1(2)$, respectively. The negative MCD bands of $\text{Co}(\text{Ph}_3\text{PO})_2\text{I}_2$ (Figure 7) at 420, 560, and 590 nm are assigned as the transitions to $^2T_2(3)$, $^2T_2(2)$, and $^2T_2(1)$, respectively. The positive MCD bands of $\text{Co}(\text{NCS})_4^{2-}$ (Figure 1) at 430, 460, and 495

nm are assigned as the transitions to $^2T_1(4)$, $^2T_1(3)$, and $^2T_1(2)$, respectively. The positive MCD bands of $\text{Co}(\text{Ph}_3\text{PO})_4^{2+}$ and $\text{Co}(\text{TBPO})_4^{2+}$ (Figures 2 and 3) at 480 nm are assigned to $^4A_2 \rightarrow ^2T_1(2)$. The MCD of $\text{Co}(\text{Ph}_3\text{P})\text{Br}_3^-$ (Figure 8) shows the apparent similarity with the MCD of $\text{Co}(\text{Ph}_3\text{PO})_2\text{Br}_2$, and we may assign the negative MCD band at 415 nm and positive MCD bands at 430, 500–515, and 560 nm as the transitions to $^2T_2(3)$, $^2T_1(4)$, $^2T_1(3)$, and $^2T_1(2)$, respectively.

The MCD spectra of the bands corresponding to spin-allowed transition $^4A_2 \rightarrow ^4T_1(P)$ of $\text{Co}(\text{Ph}_3\text{PO})_2\text{X}_2$ are very similar to those of CoX_4^{2-} . However, there are some differences between the MCD spectra of $\text{Co}(\text{Ph}_3\text{P})_2\text{X}_2$ complexes (Figure 9–12) and those of $\text{Co}(\text{Ph}_3\text{PO})_2\text{X}_2$ or CoX_4^{2-} complexes. The splitting of the band corresponding to $^4A_2 \rightarrow ^4T_1(P)$ in $\text{Co}(\text{Ph}_3\text{P})_2\text{X}_2$ is larger than those of $\text{Co}(\text{Ph}_3\text{PO})_2\text{X}_2$, and the effect of low symmetry components in the ligand field upon the transition energies seems to be important. In spite of this fact, we can not explain the MCD of $\text{Co}(\text{Ph}_3\text{P})_2\text{X}_2$ by the analysis based on the assumption that the effect of the lower symmetry field is larger than the spin-orbit coupling, as we have seen above. It seems rather better to regard the change of the MCD as a result of larger separation between E'' and $5/2U'$.

The spectra of compounds $\text{Co}(\text{Ph}_3\text{P})_2\text{X}_2$ showed a significant variation from solvent to solvent. The MCD and absorption spectra of $\text{Co}(\text{Ph}_3\text{P})_2\text{Cl}_2$ in solvents such as acetone, dichloromethane, nitromethane, and dimethylformamide (DMF) are shown in Figure 18. It seems that the triphenylphosphine compounds are very sensitive to their environment. The spectra of the other compounds in organic solvents of relatively weak basicity were essentially the same with those of the solids. Cotton and his coworkers studied the visible spectra of $\text{Co}(\text{Ph}_3\text{P})_2\text{X}_2$ and observed no significant difference between reflectance spectra and the absorption spectra of the solution in dichloromethane.¹⁹ Therefore, we used dichloromethane as a solvent for all cobalt(II) compounds appeared in this article.

MCD spectra of the charge transfer transitions in CoBr_4^{2-} and CoI_4^{2-} were reported by Bird and his coworkers.⁹ We have also observed the MCD spectra of the charge transfer transitions in $\text{Co}(\text{Ph}_3\text{PO})_2\text{I}_2$, $\text{Co}(\text{Ph}_3\text{P})_2(\text{SCN})_2$, $\text{Co}(\text{Ph}_3\text{P})_2\text{I}_2$, and $\text{Co}(\text{Ph}_3\text{P})\text{Br}_3^-$. Some of these MCD spectra are very similar to those observed in tetrahalide cobalt(II) complexes, but some are different in the sign of $[\theta]_M$. It seems that the MCD spectra will provide us with valuable information about the charge transfer transitions and will be useful to obtain the precise assignment. However, more theoretical work and the spectra over a wide range of temperature are needed.

Acknowledgment. This work was partially supported by a Scientific Research Grant from the Ministry of Education of Japan.